# Prediction of susceptibility-induced artefacts for prospective motion correction

**R. Boegle[1], J. Maclaren[1], and M. Zaitsev[1]**

[1]Dept. of Diagnostic Radiology, Medical Physics, University Hospital Freiburg, Freiburg, Germany

**Introduction**: Today's state-of–the-art MR techniques, such as real-time fMRI, are limited in their applicability and the achievable quality of the acquired images by subject motion and $B_0$ field inhomogeneities. In this work, we combine two methods to help overcome these limitations. The goal is to eventually be able to predict, and correct for, susceptibility-induced image distortions.

**Theory and Methods:** In this work, two existing techniques are combined: prospective motion correction using an external motion tracking device [1]; and a fast calculation method for $B_0$ field inhomogeneity caused by an arbitrary distribution of magnetic susceptibility [2-4].

We constructed an asymmetrical phantom (Fig.1), made entirely from PVC. It consists of a hollow cylinder containing compartments filled with MR-visible substances of various susceptibilities. A PVC table was designed and constructed to enable accurate manual rotations of the phantom during scanning for comparison with the tracking system. To demonstrate the artefacts originating from changes in $B_0$ field inhomogeneity due to object rotation, we took three rotation-corrected echo planar images (Fig. 2a-c) of the custom-made phantom: the first after shimming; the second with the shim settings of the first, but the phantom rotated by 20°; and the third after reshimming for the rotated phantom. The distortions in Fig.2a-c, illustrate the need to account for rotation-induced changes in field inhomogeneities.

To simulate the $B_0$ field, we model the phantom as a susceptibility distribution and therefore require the susceptibilities of the materials used. To measure these, we used large cylinders and cylindrical tubes filled with samples of the liquids used in the phantom. The tube lengths were 10 times longer than their radii to approximate infinitely long cylinders. The magnetic fields that are produced when placing them perpendicular to the $B_0$ field, while having them surrounded by water as a reference, were calculated analytically and then fitted to measured field maps by using an optimization method. This gave a good estimation of the susceptibilities in question. These are listed in Fig. 1 for each compartment.

We assume linear media ($\chi = M/H$), with small susceptibilities, which is common for biological tissues (with $\chi$ on the order of ppm). We therefore made a first order perturbation to Maxwell's magneto-static equations, which were then solved using Fourier transformations, as shown in [2], to give the macroscopic field. Needing the local field we have to account for the discrete nature of the nuclei encountered at the MR relevant microscopic level. As has been shown in [5], one can correct the field appropriately by using the concept of the Lorentz susceptibility cavity also known as "the Sphere of Lorentz". With this, the resulting approximation for the $B_z$ component ($B_x$ and $B_y$ are negligible for MR) of the induced difference field in k-space becomes

$$\Delta\tilde{B}_0^z(\mathbf{k}) = B_0\left[\frac{1}{3} - \frac{k_z^2}{k_x^2 + k_y^2 + k_z^2}\right]\cdot\tilde{\chi}(\mathbf{k})$$

Inverse Fourier transformation yields the field distribution in image-space.

All experiments were performed on a Magnetom Trio 3T System (Siemens medical Solutions, Germany). For empirical validation of our field simulation we used a standard gradient echo field mapping sequence (TR=250 ms, TE1=9.84 ms, TE2=12.3 ms) with an excitation angle of 25°. It is also important to account for the inevitable sample-independent intrinsic field inhomogeneities of the MR system. We therefore shimmed using a spherical oil phantom, as the magnetisation inside a spherical object is zero and therefore any measured inhomogeneities inside it are due only to the intrinsic field inhomogeneities. As expected, the measured field variations within the spherical phantom proved to be very small and could be accounted for by spherical harmonic shims. It was also important to account for the PVC table in the model, because it introduced major field inhomogeneities.

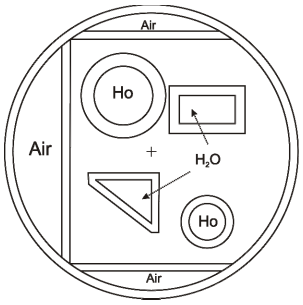


Fig. 1: Diagram of the custom-made phantom with the substance within each compartment labeled.

Susceptibilities used:
$\chi(H_2O,\text{distilled}) = -9\text{ppm}$
$\chi(\text{air}) = 0.36\text{ppm}$
$\chi(\text{holmium solution}) = -4.7\text{ppm}$
$\chi(\text{PVC}) = -10.7\text{ppm}$.

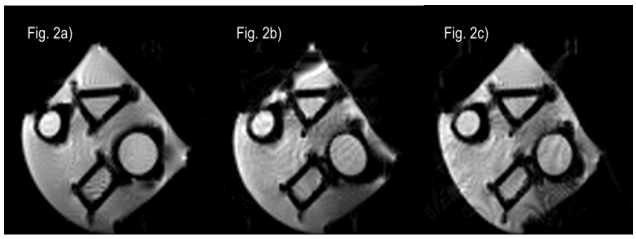


Fig. 2: EPI images where object rotation of 20° was corrected but susceptibility artefacts remain: (a) directly after shimming, (b) after a rotation (c) after a rotation and reshimming.

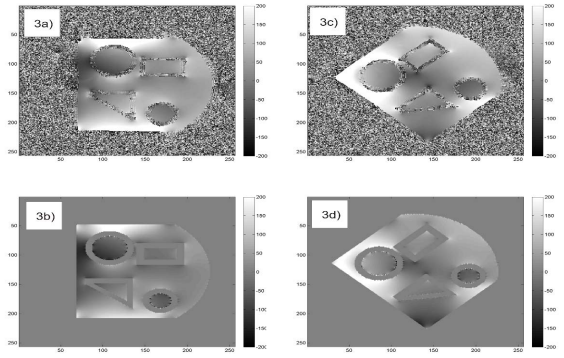


Fig. 3: A comparison between acquired (a and c) and simulated (b and d) field maps at rotation angles of 0° (a and b) and 45° (c and d).

**Results and Discussion:**

Fig. 3 compares measured and simulated field maps for two different orientations of the phantom. A good agreement between measurements and simulations is apparent. Given a susceptibility model of a human head, changes in subject position could be accounted for by rotating and translating the susceptibility distribution used and calculating the new field inhomogeneity. Thus, it would be possible to apply this approach to dynamic shimming applications where conventional (static) shimming can not account for patient motion. A second application is distortion correction for imaging techniques such as EPI used in real-time fMRI, where 3D $B_0$ maps are needed for each position in the time course.

**Conclusion:** This predictive method is an important first step towards quantifying, and suppressing or correcting susceptibility-induced distortions in prospective motion correction.

**References**: [1] Zaitsev et al., Neuroimage 2006;31(3). [2] Salomir et al., Concepts Magn. Reson. B 19. [3] Marques et al., Concepts Magn. Reson. B 25. [4] Koch et al., Phys. Med.Biol. 51 (2006). [5] Durrant et al., Concpts Magn. Reson. 18A (1).

**Acknowledgements:** This work is a part of the INUMAC project supported by the German Federal Ministry of Education and Research, grant #01EQ0605 and the "Real-time motion tracking and correction for MR and Spectroscopy" project supported by NIDA (1R01 DA021146).